# DYNAMIC FINITE ELEMENT AND DYNAMIC PHOTOELASTIC ANALYSES OF AN IMPACTED PRETENSIONED PLATE

A. S. Kobayashi, S. Mall and A. F. Emery*

## INTRODUCTION

Two popular test specimens used in studying crack arrest potential of structure steel are the ESSO and Robertson specimens [1,2] in which dynamic crack propagation is initiated through impacting a wedge in the crack of a subcritically loaded single-edged notch tension plate. Crack arrest is achieved by regions of either higher fracture toughness generated by higher local temperature in low carbon steel specimen and/or lower stress intensity factors generated by lower local stress field.

Dynamic photoelastic analysis of ESSO type test specimens modeled by Homalite-100 plates [3] show that the dynamic effects of the propagating crack combined with that of the impacting projectile have considerable effect on the dynamic stress intensity factor and hence on crack propagation. Unfortunately, these results neither provide a unique relation between the crack velocities and dynamic fracture toughness nor a definitive conclusion regarding the basic mechanism of crack arrest. In addition, the results are not in complete agreement with the more recent experimental results obtained on thicker Homalite-100 plates [4,5].

In order to verify, by an independent procedure, some of the controversial results obtained during our past seven-year efforts in fracture dynamics, the authors have used a relatively simple dynamic finite element code to duplicate some of their past work in dynamic photoelasticity [6,7,8]. Encouraged by the reasonable agreements between the numerical and experimental results obtained through this series of studies involving single-edged notch specimens loaded to criticality, the same dynamic finite element code was used to analyze the previous dynamic photoelastic results on the ESSO type test specimens [3].

## DYNAMIC PHOTOELASTIC ANALYSIS

The dynamic photoelastic experiments in this paper involve subcritically loaded single-edged notch tension specimens where crack propagation was initiated by an impacted flat-nosed projectile or a 65° wedge. The test specimens consisted of a 9.53mm thick Homalite-100 plate with a 0.254 x 0.254m test section loaded in a fixed gripped condition with uniform grip displacement, and with a single-edged starter crack approximately 9.53mm in length. The dynamic properties of Homalite-100 were obtained following the procedure of Clark and Sanford [9], which yielded an average dynamic modulus of elasticity, Poisson's ratio and stress optic coefficient of 4.65 GPa, 0.345 and 27.15 MPa-mm/fringe, respectively. The averaged static fracture toughness, which was obtained through separate tests using SEN specimens, was 0.64 $MPa \cdot m^{1/2}$.

*University of Washington, Department of Mechanical Engineering, Seattle, Washington 98195, U.S.A.

Dynamic stress intensity factors, $K_D$, were determined by Bradley's two parameter procedure [10] and the dynamic energy release rate, $\mathcal{G}_D$, was computed using Freund's equation [11] from the dynamic stress intensity factors. Further details of these data reduction schemes can be found in references [6] and [8].

## DYNAMIC FINITE ELEMENT ANALYSIS

The dynamic finite element code, Hondo [12], used in this investigation is based on an explicit time integration scheme and constant strain quadrilateral elements. The crack tip motion was modeled by discontinuous jumps where crack tip moved from one finite element node to another at discrete time intervals. This discrete propagation of the crack tip generated significant oscillations in the states of stress and displacement surrounding the crack tip. The numerical noise was filtered by computing directly the dynamic energy released by the discrete crack tip advancement from the time averaged normal stress ahead of the advancing crack tip and the corresponding time-averaged crack opening displacement after crack advance. Details of this numerical procedure as well as an accuracy check of the procedure are described in reference [6].

Figure 1 shows the finite element breakdown involving a total of 532 elements and 585 nodes used in this analysis. Impacted wedge-loading was simulated by two simultaneously applied vertical and horizontal forces at the crack mouth without the wedge-shape and the impact forces for the flat nose projectile and 65° wedge were assumed to vary with impact duration. Large plastic deformations at the impact sites were assumed to dissipate about 66 percent and 43 percent of the impact energies for the flat nose and 65° wedge impacts, respectively. Estimates of these energy losses as well as impact durations were made by comparing the calculated dynamic maximum shear stress patterns of a given impulse with the associated dynamic isochromatic patterns as shown in Figure 2.

## PRETENSIONED SINGLE-EDGED NOTCH PLATE IMPACTED BY FLAT NOSE PROJECTILE

In the series of dynamic photoelastic experiments reported in reference [3], the crack propagated in some pretensioned single-edged notch plates while it did not run in others. These stop-or-go results potentially provided information for estimating the static fracture toughness under stress-wave loadings but unfortunately the dynamic photoelastic patterns prior to crack propagation were not recorded in these experiments. A combination of dynamic finite element analysis and dynamic photoelasticity results provided a procedure in which the dynamic state prior to triggering of the dynamic polariscope could be estimated by some trial and error. Table 1 shows such maximum dynamic stress intensity factors due to impact for the stationary crack in Test No. W012172 and prior to crack propagation in Test Nos. W020672 and W090711.

It is interesting to note that this combined dynamic photoelastic-dynamic finite element analysis results in Table 1 indicate that the dynamic fracture toughness, $K_c$, under this combined static and stress wave loadings is close to, within experimental scatters, the static fracture toughness of $K_c = 0.64\ \text{MPa}\cdot\text{m}^{1/2}$. Perhaps such coincidence may be expected in view of the recent work by G. C. Smith [13] who found that the variations in fracture toughness of 4.76mm thick Homalite-100 plates is approximately equal to the static fracture toughness for the time interval to failure of 20 microseconds. The 30-50 percent increase in stress intensity





factor due to impulse loading falls within the rapidly changing dynamic fracture toughness at this time interval to failure.

## PRETENSIONED SINGLE-EDGED NOTCH PLATE IMPACTED BY A 65° WEDGE

The dynamic photoelasticity record of Test No. W012472 was analyzed then by the dynamic finite element method using the idealized crack velocity shown in Figure 3. Figure 4 shows a comparison of the dynamic energy release rates due to static preload on the specimen. The rapid fluctuations in the FEM results at an approximate crack length of a/b = 0.15 is due to the momentary drop in crack velocities at this location. Otherwise good agreement between the measured and computed dynamic energy release rate are noted.

## DISCUSSION

Our conclusion that fracture toughness, which did not differ with its static counterpart, under the combined static and impulse loadings is in agreement with that discussed in reference [7] involving simulated dynamic tear tests. As mentioned previously, these findings are in agreement with those in reference [13] because of the relatively low strain rate effects in these tests.

The dynamic energy release rate at crack arrest was much lower than those measured in non-impact experiments [7] which again reinforces our postulate that $\mathcal{G}_D$ at crack arrest is not a material property. The average dynamic energy release rate, which is obtained by dividing the sum of the total dynamic energy release rates by the newly created crack surface by crack propagation, for Test W012472, yielded $\mathcal{G}_{D]ave}/\mathcal{G}_c = 2.33$ and 2.28 from the dynamic photoelasticy and dynamic FEM analysis, respectively. The large $\mathcal{G}_{D]ave}$ generated by elastic analysis for a prescribed crack propagation history probably indicates the larger dissipation in dynamic energy due to viscous damping and at the flexible edge grips under high impact loading.

## ACKNOWLEDGEMENT

The results reported in this paper were obtained in a research contract funded by the Office of Naval Research under Contract No. N00014-76-C-0060 NR 064-478. The authors wish to acknowledge the continuous support and encouragement of Drs. N. R. Perrone and N. Basdegas of ONR.

## REFERENCES

1. BLUHM, J. L., Fracture, ed. H. Liebowitz, Vol. V, Academic Press, 1969, 1-63.
2. KANAZAWA, T., Dynamic Crack Propagation, ed. G. C. Sih, Noordhoff International, 1973, 565-597.
3. KOBAYASHI, A. S. and WADE, B. G., ibid loc cit, 663-677.
4. KOBAYASHI, T. and FOURNEY, W. L., Proc. of 12th Annual Meeting of the Society of Engineering Sciences, University of Texas at Austin, Oct. 20-22, 1975, 131-140.

5. KOBAYASHI, T. and DALLY, J. W., "The Relation Between Crack Velocity and the Stress Intensity Factor in Birefringenet Polymers", presented at ASTM Symposium on Fast Fracture and Crack Arrest, Chicago, Illinois, June 28-30, 1976.
6. KOBAYASHI, A. S., EMERY, A. F. and MALL, S., "Dynamic Finite Element and Dynamic Photoelastic Analyses of Two Fracturing Homalite-100 Plates", to be published in Experimental Mechanics.
7. KOBAYASHI, A. S. and MALL, S., Proc. of the Int. Conf. on Dynamic Eracture Toughness, London, July 5-7, 1976, 259-272.
8. KOBAYASHI, A. S., EMERY, A. F. and MALL, S., Presented at the ASTM Symposium on Fast Fracture and Crack Arrest, Chicago, Illinois, June 28-30, 1976.
9. CLARK, A. B. J. and SANFORD, R. J., Proc. of the Soc. for Experimental Stress Analysis, Vol. 20, No. 2, 1973, 148-151.
10. BRADLEY, W. B. and KOBAYASHI, A. S., Engineering Fracture Mechanics, Vol. 3, 1971, 317-332.
11. FREUND, L. B., J. of Mechanics and Physics of Solids, Vol. 20, 1972, 141-152.
12. KEYS, S. W., Sandia Laboratories Report SLA-74-0039, April 1974.
13. SMITH, G. C., PhD thesis submitted to California Institute of Technology, April 1975.


Table 1 Dynamic Stress Intensity Factor Prior to Crack Propagation in an Impacted Pretensioned Plate

| Test No. | Prescribed Displacement $u_{top}$ $u_{bottom}$ | Projectile Velocity | Stress Intensity Factor Due to Pre-loading | Dynamic Stress Intensity Factor Due to Impact at 20 μsec* | Resultant Stress Intensity Factor | Remarks |
|---|---|---|---|---|---|---|
| W012172 | 0.0572 mm<br>0.0572 mm | Flatnose,<br>12.34 gm<br>24 m/sec | 0.30<br>MPa·m$^{1/2}$ | 6.41<br>MPa·m$^{1/2}$ | 0.70<br>MPa·m$^{1/2}$ | Crack did not run |
| W020672 | 0.0254 mm<br>0.0762 mm | Flatnose,<br>12.34 gm<br>46 m/sec | 0.40<br>MPa·m$^{1/2}$ | 0.40<br>MPa·m$^{1/2}$ | 0.80<br>MPa·m$^{1/2}$ | Crack ran |
| W090771 | 0.0889 mm<br>0.0889 mm | Flatnose,<br>12.34 gm<br>26 m/sec | 0.47<br>MPa·m$^{1/2}$ | 0.40<br>MPa·m$^{1/2}$ | 0.87<br>MPa·m$^{1/2}$ | Crack ran |

$K_c$ = 0.64 MPa·m$^{1/2}$

*Dynamic S.I.F. for same impact pulse, regardless of differences in muzzle velocity.





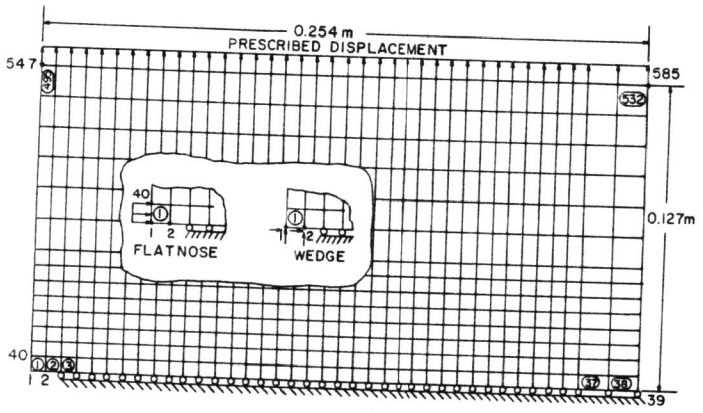


Figure 1 Finite Element Breakdown with Applied Impact Forces in Flatnose and 65° Wedge Projectile

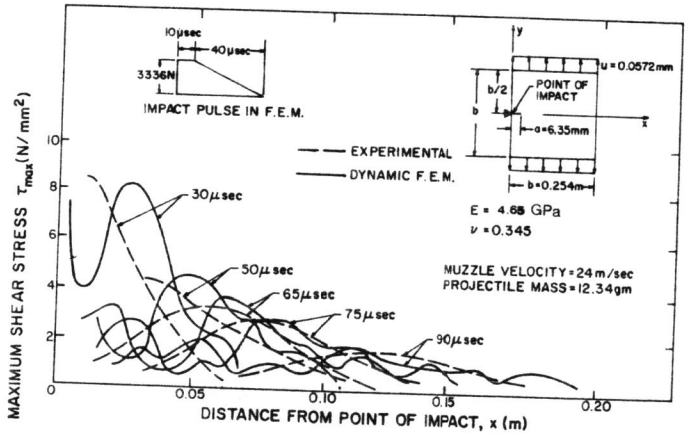


Figure 2 Dynamic Maximum Shear Stresses Along the Axis of Symmetry in Single-Edged Crack Pretensioned Plate Impacted by a Flatnose Projectile, Test No. W012172

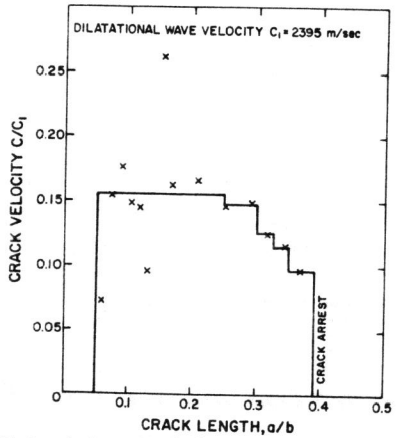


Figure 3 Crack Velocities Used for Numerical Analysis Along with Experimental Data, Test No. W012472

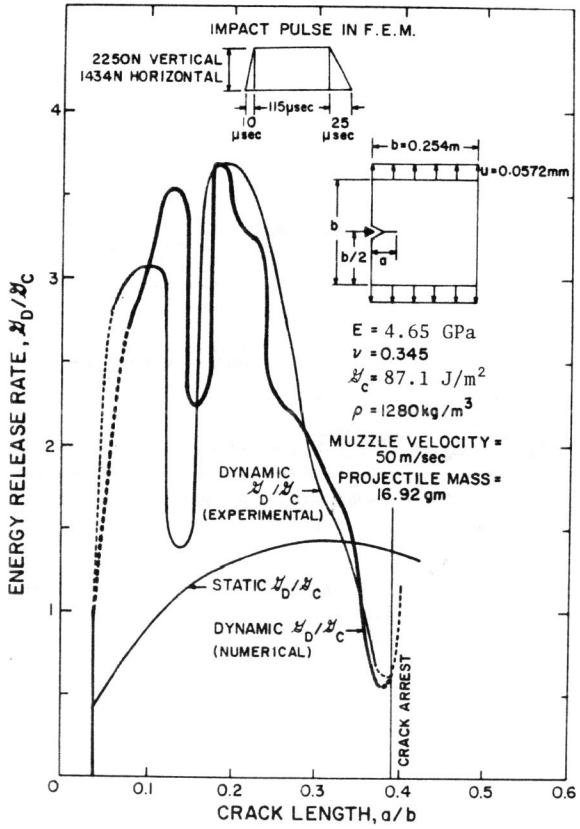


Figure 4 Energy Release Rates in a Single-Edged Crack Pretensioned Plate Impacted by a 65° Wedge, Test No. W012472